

Mercury's magnetopause and bow shock from MESSENGER observations

Reka Moldovan (1), Brian J. Anderson (2), Catherine L. Johnson (1,3), James A. Slavin (4), Haje Korth (2), Michael E. Purucker (4), Sean C. Solomon (5)

(1) University of British Columbia, Vancouver, British Columbia, Canada V6T 1Z4; (2) The Johns Hopkins University Applied Physics Laboratory, Laurel, MD 20723, USA, (3) Planetary Science Institute, Tucson, AZ 85719, USA (4) NASA Goddard Space Flight Center, Greenbelt, MD 20771, USA; (5) Department of Terrestrial Magnetism, Carnegie Institution of Washington, Washington DC 20015, USA (rmoldova@eos.ubc.ca).

1. Introduction

Mercury's bow shock and magnetopause have been modeled from Mariner 10 [1] and MErcury Surface, Space ENvironment, GEOchemistry, and Ranging (MESSENGER) flyby observations [2]. A conic section is adopted for the bow shock [1] and an arctangent function for the magnetopause [3]. The models show that the bow shock is more flared than at Earth but the shape of the magnetopause is similar to Earth's, with a subsolar stand-off distance of 1.4 R_M (R_M is Mercury's radius). We improve on these models using magnetic field data from Mercury orbit.

2. Observations

Magnetopause and bow shock crossings identified from the first six months of orbital observations are used in the analysis. Identification of the magnetopause boundary is on the basis of rotation of the magnetic field toward (away from) the planetary field on the inbound (outbound) crossing. In cases with low magnetic shear, which makes identification difficult, the temporal variability of the field, measured in the 1-10 Hz bandpass fluctuation amplitude (B_{AC}), is used to identify the outer edge of the magnetopause boundary, and a subsequent decrease in B_{AC} is assumed to mark the inner edge of this boundary. The bow shock is identified from a sharp increase (decrease) in the total field magnitude on the inbound (outbound) leg of the orbit. During parallel shock conditions (when IMF $B_x \gg B_y, B_z$), the bow shock is difficult to identify and is usually preceded (succeeded) by strong foreshock waves upstream of the inbound (outbound) crossing. As multiple bow shock and magnetopause crossings are observed on almost every pass, outer and inner crossings are identified for both the bow shock and magnetopause. For model fits, we used the mean

time between the outer and inner boundary as the crossing time.

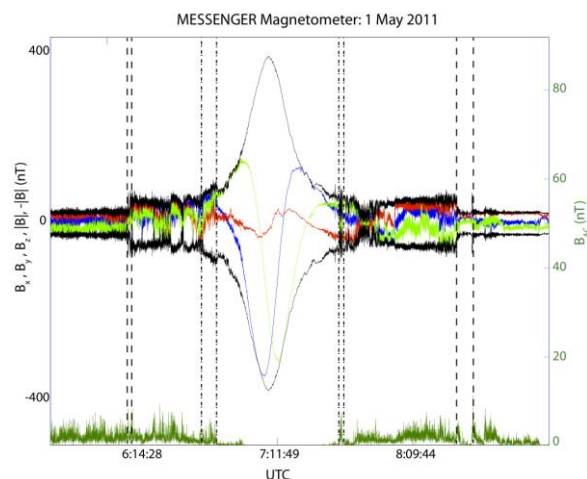


Figure 1: Bow shock and magnetopause crossings on 1 May 2011. Lines indicate inner and outer bow shock crossings (dashed) and inner and outer magnetopause crossings (dot-dashed). The scale for B_{AC} (dark green) is on the right; that for B_x (red), B_y (green), B_z (blue), and $|B|$ (black) is on the left.

3. Magnetopause Fits

Magnetopause crossings were modeled with a paraboloid shape and the Shue model [4] in r - x space, where $r = \sqrt{y^2 + (z - z_d)^2}$, and z_d is the 472 km northward offset of the dipole from the Mercury solar orbital (MSO) coordinates [5]. For the paraboloid model, crossings were fit to

$$x(r) = -\left(\frac{\gamma^2 + 1}{4R_{ss}}\right)r^2 + R_{ss}, \quad (1)$$

where γ is a flaring parameter and R_{ss} is the subsolar magnetopause distance [6]. γ and R_{ss} were determined for each pass and averaged, giving $R_{ss} = 1.89 R_M$ and $\gamma = 1.74$. Any value of $\gamma > 1$ is physically unreasonable because it gives a subsolar distance that is not the minimum distance to the magnetopause. Setting $\gamma = 1$, we find $R_{ss} = 1.5 R_M$ and use this as our best-fit paraboloid (Figure 2).

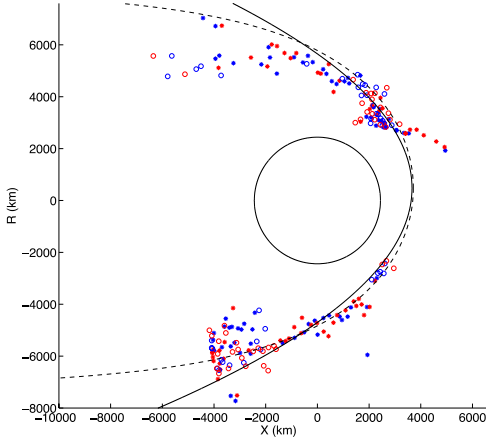


Figure 2: Magnetopause crossings color-coded according to IMF B_z (blue > 0 , red < 0) and IMF B_x (stars > 0 , circles < 0). The best-fit paraboloid to the data (black) is given by $R_{ss} = 1.50 R_M$ and $\gamma = 1.00$. The Shue model fit to the data (dashed black) has parameters $R_{ss} = 1.52 R_M$ and $\alpha = 0.52$.

We also used the Shue model [4] given by:

$$x(r, \theta) = \sqrt{R_{ss}^2 \left(\frac{2}{1 + \cos \theta} \right)^{2\alpha} - r^2}, \quad (2)$$

The angle θ is given by $\theta = \tan^{-1} \left(\frac{r}{x} \right)$, and α is also a flaring parameter that governs whether the magnetopause is closed ($\alpha < 0.5$) or open ($\alpha > 0.5$) on the night side. The average curve from fits to individual passes yields $R_{ss} = 1.45 R_M$ and $\alpha = 0.51$.

4. Bow Shock Fits

The bow shock crossings were modeled by a conic section given by [2]:

$$\sqrt{(x - x_0)^2 + r^2} = \frac{L}{1 + \varepsilon \cdot \cos \theta}, \quad (3)$$

The best-fit parameters are given by $x_0 = 0.5 R_M$, $\varepsilon = 1.07$, and $L = 2.7 R_M$ (Figure 3).

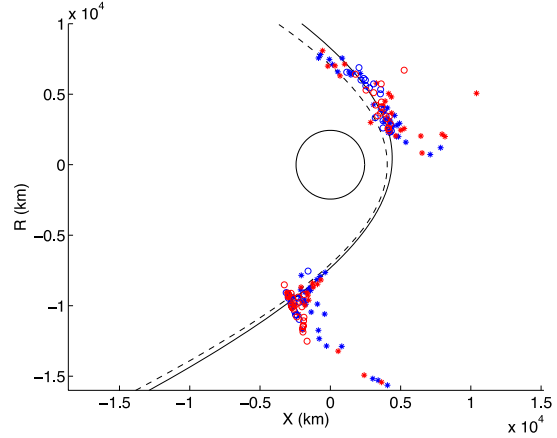


Figure 3: Bow shock crossings color-coded as in Figure 2. The dashed line is the Slavin et al. [2] model, and the solid line is a modified version, with $L = 2.7 R_M$ and an offset along the z -axis of 472 km that provides an improved fit to these data.

6. Summary

Thus far, there is no clear correlation between magnetopause shape or size and interplanetary magnetic field (IMF) B_z direction. However, there does seem to be a correlation between the R_{ss} value and IMF B_x direction. As seen in Figure 2, most of the magnetopause crossings with large x distances correspond to a sunward IMF orientation. For the magnetopause, both our paraboloid and Shue model fits yield larger subsolar stand-off distances than that found earlier [2]. Our bow shock model is in good agreement with earlier results [2] after translation of the data into the offset magnetic coordinate system, although there are some anomalous crossings, particularly in the outbound bow shock. A minimum variance analysis is being conducted to establish the magnetopause boundary normals and place bounds on the dayside reconnection efficiency at Mercury.

References

- [1] Slavin, J. A. and Holzer, R. E., JGR, 86, 11401, 1981.
- [2] Slavin, J. A., et al., GRL, 36, L02101, doi:10.1029/2008GL036158, 2009.
- [3] Howe, H. C. and Binsack, J. H., JGR, 77, 3334, 1972.
- [4] Shue, J.-H., et al., JGR, 102, 9497, 1997.
- [5] Anderson, B. J., this meeting, 2011.
- [6] Belenkaya, E.S. et al., PSS, 53, 863-872, doi:10.1016/j.pss.2005.03.004, 2005.

